

Single Layer Coating Photonic Crystal Fiber Biosensor based on Surface Plasmon Resonance

P Vinod Kumar, Snivash, Mohammed Fahimullah A, K Vinay Gokul

Abstract: This paper is a demonstration for the design of photonic crystal fiber biosensor which is based on the phenomenon of surface plasmon resonance. The plasmonic coating covers the outer layer of the Photonic Crystal fiber to ease the fabrication process, we choose Gold. To quantitatively measure the represented design, we utilize a technique called as the Finite element method (FEM). To accomplish the sensitivities of 4300nm/RIU and 408.468 RIU⁻¹ we apply the methodologies of wavelength and amplitude interrogation models. This design yielded a resolution of 2.33×10⁻⁵ respectively. A fluctuation from 1.33 to 1.39 in the analyte refractive index can be identified and measured by this design. The sensing range of the design is wide and may also be used in biological detection.

Keywords: Biosensor, Resolution, PCF, SPR

I. INTRODUCTION

In recent trends, there's a keen interest for the study of Surface plasmon resonance effect based Photonic Crystal Fiber because of its good properties and its advantages. SPR based PCF has been used for physical, biological, chemical applications. It is very important to choose the proper design and plasmonic material. The sensor performance is dependent on the proper selection of plasmonic material. Several kinds of plasmonic material have been used. The most common type of plasmonic material is being used is Gold because of its properties which includes chemically stability, oxidation and it exhibits high sensitivity because of the large resonance peaks when compared with other plasmonic metals [7]. When SPR based PCF are compared with fiber-based sensors, the former provides more sensitivity and resolution when compared with the latter. Several designs have been proposed by researchers in the past few years for different applications. Md Hasan [3] proposed an extremely sensitive PCF based on Surface Plasmon Resonance which showed wavelength sensitivity up to 2200nm/RIU 1.33 to 1.36. Azzam [1] proposed a biosensor based on SPR whose sensitivity was 2400nm RIU⁻¹ in visible or near IR region. A square array PCF based SPR refractive index was proposed by Liu [8] had a remarkable sensitivity up to 7250nm/RIU⁻¹ in the range of 1.38 - 1.42 and it had a

Revised Version Manuscript Received on Jun 20, 2019.

P Vinod Kumar, Electronics and Communication Engineering, SRM Institute of Science and Technology, Chennai, India.

S Nivash, Electronics and Communication Engineering, SRM Institute of Science and Technology, Chennai, India.

Mohammed Fahimullah A, Electronics and Communication Engineering, SRM Institute of Science and Technology, Chennai, India.

K Vinay Gokul, Electronics and Communication Engineering, SRM Institute of Science and Technology, Chennai, India.

good resolution of 138×10⁻⁵. Li [5] proposed a multi-coating PCF with SPR at near wavelength for detecting higher RI. In this paper the plasmonic material has been coated internally which is a tedious process in real time. So, for ease fabrication gold layer has been coated outside the PCF in our paper. WeiquanSu[6] proposed a D-shaped symmetrical dual PCF which showed a high resolution up to 6.82 × 10⁻⁶ in the range of 1.36 - 1.41. The important measures of the sensor performance are to make the fabrication easy and comfortable. The proposed PCF biosensor design has a simple structure and is easier to fabricate using the stack and draw [4] process.

II. THEORETICAL MODELLING

Fig.1 represents the two-dimensional illustration of the preferred single layer PCF biosensor. This presented design was designed using COMSOL Multiphysics. Fiber design is characterized by its parameters pitch (Λ) and diameter (d₁, d₂). The Λ denotes the measure between the core of air holes, also d₁ and d₂ are the diameters of the smaller and bigger circles respectively. The value for these parameters is Λ = 2μm, d₁ = 0.25 × Λ, and d₂ = 0.5 × Λ. A small hole in the core of the fiber is introduced, and its diameter is given as d_c = 0.15 × Λ and the thickness of the plasmonic material is t_{au} = 30nm. The thickness of the analyte region on top of the gold layer is t_{Anal} = 0.8μm. Perfectly Matched Layer is the external layer of the entire structure is used to absorb the electromagnetic radiations.

The number of degrees of freedom of a computed mesh generation is 102587 and the number of elements is 19938. The photonic crystal fiber is made up of Silica. The refractive index of the fiber which is made using Silica can be calculated using Sellmeier equation [3] is:

$$n^2(\lambda) = 1 + \frac{B_1 \lambda^2}{\lambda^2 - c_1} + \frac{B_2 \lambda^2}{\lambda^2 - c_2} + \frac{B_3 \lambda^2}{\lambda^2 - c_3}$$

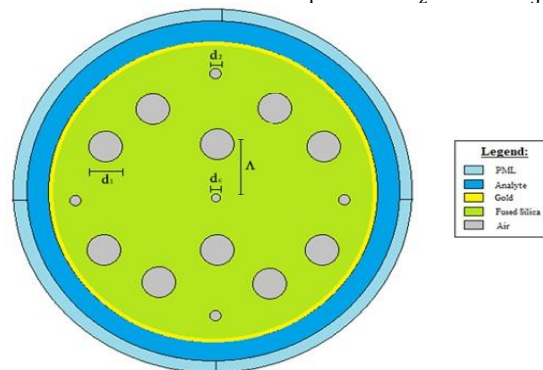


Fig. 1. The cross-sectional view of the proposed PCF sensor whose parameters are Λ = 2μm, d₁ = 0.25 × Λ and d₂ = 0.5 × Λ and d_c = 0.3 × Λ.

where n is RI of silica at wavelength l in microns. B_1, B_2, B_3 and c_1, c_2, c_3 are Sellmeier coefficients whose values are given by 0.696166300, 0.407942600, 0.897479400 and 4.67914826103 $\mu m^2, 1.35120631102 \mu m^2, 97.9340025 \mu m^2$ respectively. The permittivity of gold is obtained using dielectric function of gold using Drude-Lorentz [3] given as:

$$\epsilon_{Au} = \epsilon_{\infty} - \frac{\omega_D^2}{\omega(\omega + j\gamma_D)} - \frac{\Delta\Omega_L^2}{(\omega^2 - \Omega_L^2) + j\Gamma_L\omega} \quad (2)$$

where the permittivity (ϵ_{∞}) of gold at high frequencies is 5.9673. $\omega_D, \gamma_D, \omega, \Omega_L$ parameters are explained in [7].

III. SIMULATION RESULTS

The parameters of the Photonic Crystal Fiber determines the Sensor performance. The evanescent field gets originated from the core and when this field hits the gold (plasmonic metal) surface plasmon waves are produced in the metal-dielectric interface. There is a particular wavelength called resonant wavelength at which the highest energy from fundamental mode gets transferred to the plasmonic mode and hence a sharp peak in the loss curve can be observed as shown in Fig.3.

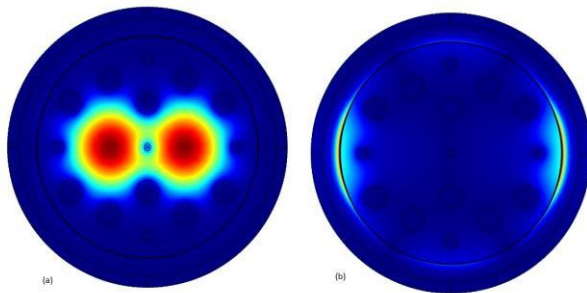


Fig. 2. Mode field distribution at (a)Fundamental mode and (b)Plasmonic mode for analyte RI=1.36 and the parameters of PCF include $\Lambda=2\mu m, d1=0.25 \times \Lambda, d2=0.5 \times \Lambda, dc=0.3 \times \Lambda$ and $t_{au}=30 \text{ nm}$.

By using the change in the loss peak the refractive index of an analyte can be determined. X-polarization loss is very less when compared to Y-polarization loss, only Y-polarization was considered throughout the simulation. Fig.2(a) represents the Fundamental mode Electric field distribution for analyte refractive index 1.36 and 2(b) represents the distribution of the electric field of fundamental mode for analyte RI index 1.36. From Fig[2a] and Fig.[2b] it can be understood that the electric field which has been originated from the core in Fig[2a] reaches the plasmonic material in Fig[2b].

The confinement loss which is expressed in dB/cm can be calculated using [9]:

$$\alpha(\text{dB/cm}) = 8.686 \times k_0 \times \text{Im}(n_{eff}) \times 10^4 \quad (3)$$

where $k_0=2\pi/\lambda$ represents the free space propagation constant, λ represents the wavelength which is expressed in μm and $\text{Im}(n_{eff})$ represents effective refractive index imaginary part(n_{eff}).

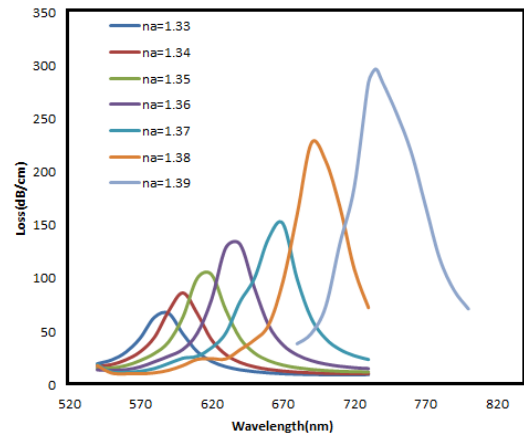


Fig. 3. Fundamental loss curve for analyte RI fluctuating from 1.33 to 1.39. The PCF parameters include $\Lambda=2\mu m, d1=0.25 \times \Lambda, d2=0.5 \times \Lambda, dc=0.3 \times \Lambda$ and $t_{au}=30 \text{ nm}$.

There is always a shift in the loss depth whenever the RI of the analyte is changed as shown in Fig.3. When the analyte refractive index is increased it leads to redshift of the curve therefore the resonant wavelength also gets redshifted. When the RI of the analyte is decreased blueshift occurs, therefore the resonant wavelength also gets blue shifted. It can be understood that the shift in the loss depth is due to the change in the analyte Refractive index. The effective refractive index of the plasmonic mode is dependent on change of analyte refractive index. The resonant Wavelength for analyte RI of 1.33, 1.34, 1.35, 1.36, 1.37, 1.38, 1.39 is 590nm, 600nm, 620nm, 640nm, 670nm, 692nm, 735nm and its corresponding losses are 66.785dB/cm, 86.049554dB/cm, 103.4302dB/cm, 13.0524dB/cm, 151.384dB/cm, 228.335dB/cm, 29.8218dB/cm. Whenever there is a change in the RI of the analyte, resonant wavelength always gets shifted either towards the higher wavelength or towards the lower wavelength. The sensor's Sensitivity based on wavelength methodology is dependent on the resonant wavelength shift.

The wavelength Sensitivity S_{λ} which is expressed in nm/RIU can be calculated using,

$$S_{\lambda}(\text{nm/RIU}) = \Delta\lambda_{peak} / \Delta n_a \quad (4)$$

where Δn_a represents the analyte RI changes and $\Delta\lambda_{peak}$ represents the difference of the successive resonant peaks. The resonant wavelength shift of 10, 20, 20, 30, 22, 43 for analyte RI value carried in the range of 1.33 to 1.39 with an increment of 0.01. By using equation the wavelength sensitivities are 1000, 2000, 2000, 3000, 2200, 4300 nm/RIU respectively. The average wavelength sensitivity for analyte RI range 1.33-1.39 is 2616 nm/RIU. To indicate the performance of the sensor, there is a parameter called Resolution can be calculated which is expressed in RIU using [2]:

$$R(\text{RIU}) = \Delta n_a \times \Delta\lambda_{min} / \Delta\lambda_{peak} \quad (5)$$

Where $\Delta\lambda_{peak}$ and $\Delta\lambda_{min}$ represent the difference of the successive resonant wavelength and the minimum spectral resolution. Assume $\Delta\lambda_{min}$

=0.1nm, $\Delta n_a = 0.01$ and the calculated $\Delta\lambda_{peak} = 43nm$.

The highest Resolution recorded for our design is 2.33×10^{-5} . So, this sensor can detect refractive index changes up to 0.00001. There is also another important parameter called Amplitude Sensitivity to measure the sensor performance. The Amplitude sensitivity S_A has been analyzed and it can be calculated which is expressed in RIU⁻¹ using,

$$S_A(RIU^{-1}) = -\frac{1}{\alpha(\lambda, n_a)} \frac{\delta(\lambda, n_a)}{\delta n_a} \quad (6)$$

Where $\delta\alpha(\lambda, n_a)$ refers to the confinement loss difference of two successive analyte RI and $\alpha(\lambda, n_a)$ is the confinement loss. For all RI change of analyte fluctuating from 1.33 to 1.39 whose RI change is in the order of 0.01, their amplitude sensitivities have been calculated and from the measured values it has been found that the maximum amplitude sensitivity has been obtained for analyte Refractive Index 1.38. The maximum Amplitude sensitivity at Refractive index of 1.38 is 408 RIU⁻¹ and this is obtained at 710nm wavelength.

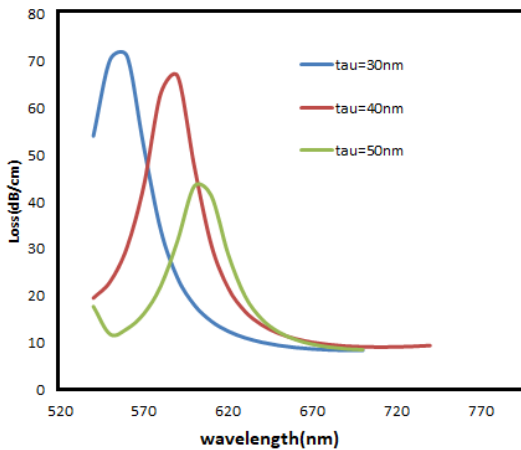


Fig. 4. loss curve for different gold thickness $t_{au}=30nm, 40nm, 50nm$ and the parameters of PCF are include $\Delta = 2\mu m, d_1=0.25 \times \Delta, d_2=0.5 \times \Delta, d_c=0.3 \times \Delta$ and $t_{au}=30 nm$.

Amplitude sensitivity and loss depth changes when there is a change in the gold thickness. So these two parameters depend on the plasmonic material thickness. The loss curve for different plasmonic thickness at analyte RI=1.38 is shown in Fig.4. The decrease in the loss depth is due to the damping effect of the gold [10]. Therefore, less energy from fundamental core mode is transferred to the plasmonic mode when compared with gold thickness of the lower value. There is also a shift in the curve when the thickness of plasmonic material (τ) is increased. When the gold thickness τ is 30nm the highest Amplitude Sensitivity which was observed was 382.3 RIU⁻¹ but when the thickness of plasmonic material was increased to 40nm then the Amplitude sensitivity increased to 408.468. When the gold thickness was increased to 50nm peak loss became comparatively less and amplitude sensitivity got reduced, so a constant thickness of gold 40nm was used throughout the

simulation. The highest Amplitude Sensitivity recorded for our design is 408.469 RIU⁻¹ at a wavelength of 710nm.

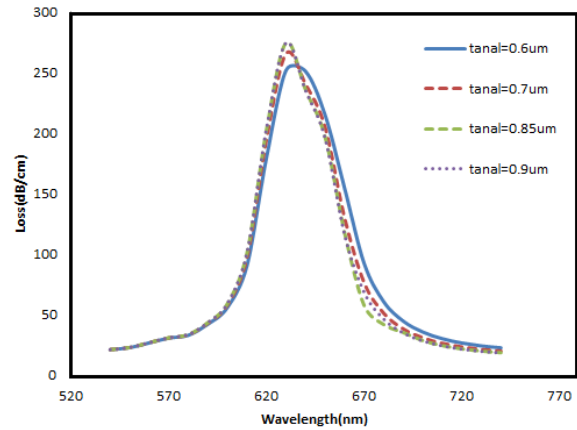


Fig. 5. Loss curve of fundamental mode for different analyte thickness $t_{anal}=0.6\mu m, 0.7\mu m, 0.85\mu m, 0.9\mu m$. and the parameters of PCF are include $\Delta = 2\mu m, d_1=0.25 \times \Delta, d_2=0.5 \times \Delta, d_c=0.3 \times \Delta$ and $t_{au}=30 nm$.

From the Fig.5 it can be understood that there is not much change in the loss depth when the thickness of the analyte is changed. The loss depth for the different analyte thickness of about 0.6nm, 0.7nm, 0.85nm is 251.041(dB/cm), 265.614(dB/cm), 274.584(dB/cm). Since there is not much difference in the loss depth as you can see in fig so constant thickness of analyte layer $t_{anal}= 0.8\mu m$ has been assumed throughout the simulation.

The different analyte RI and its following resonant wavelength graph for the different τ thickness has been plotted in Fig.6. The regression analysis has been performed for different variation in gold thickness. The regression equation for gold thickness $t_{au}=30nm$ is given by $1431.4X-1350.1$ and its corresponding R-Square values is 0.9673 and the regression equation of linear line fitting for gold thickness $t_{au}=40nm$ is $Y=2389.3x-2599.9$ and its corresponding R-Square value is 0.9695.

The R^2 value is almost nearer to unity, which indicates that the proposed sensor is linear ranging from 1.33 to 1.39. Since R^2 value is high and it is close to unity, this sensor which has been proposed by us can be implemented in practical sensing applications.

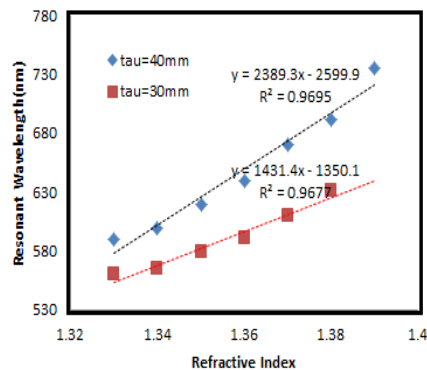


Fig. 6. Refractive index vs resonance wavelength graph for different gold layer thickness.

AUTHORS PROFILE

IV. CONCLUSION

Through this paper we represent the design of PCF biosensor built on the phenomenon of SPR. The plasmonic coating covers the outer layer of the Photonic Crystal fiber to ease the fabrication process, we choose Gold. The sensitivities of 4300nm/RIU and 408.468RIU⁻¹ can be accomplished by using the methodologies of wavelength and amplitude sensitivities. Since R² value is close to unity the sensor can be used in real time sensing applications. The proposed design could be used for biological detection and it has a wide sensing range from 1.33 to 1.39.

REFERENCES

1. Shaimaa I Azzam, Mohamed Farhat O Hameed, Rania Eid Shehata, AM Heikal, and Salah SA Obayya. Multichannel photonic crystal fiber surface plasmon resonance based sensor. *Optical and Quantum Electronics*, 48(2):142, 2016.
2. MS Aruna Gandhi, S Sivabalan, P Ramesh Babu, and K Senthilnathan. Designing a biosensor using a photonic quasi-crystal fiber. *IEEE Sensors Journal*, 16(8):2425–2430, 2016.
3. Md Hasan, Sanjida Akter, Ahmmed Rifat, Sohel Rana, and Sharafat Ali. A highly sensitive gold-coated photonic crystal fiber biosensor Multidisciplinary Digital Publishing Institute, 2017. based on surface plasmon resonance. In *Photonics*, volume 4, page 18.
4. Itaru Ishida, Tsuyoshi Akamatsu, Zhaoyang Wang, Yusuke Sasaki, Katsuhiko Takenaga, and Shoichiro Matsuo. Possibility of stack and draw process as fabrication technology for multi-core fiber. In *2013 Optical Fiber Communication Conference and Exposition and the National Fiber Optic Engineers Conference (OFC/NFOEC)*, pages 1–3. IEEE, 2013.
5. Duanming Li, Wei Zhang, Huan Liu, Jiangfei Hu, and Guiyao Zhou. High sensitivity refractive index sensor based on multicoating photonic crystal fiber with surface plasmon resonance at near-infrared wavelength. *IEEE Photonics Journal*, 9(2):1–8, 2017.
6. Chao Liu, Weiquan Su, Qiang Liu, Xili Lu, Famei Wang, Tao Sun, and Paul K Chu. Symmetrical dual d-shape photonic crystal fibers for surface plasmon resonance sensing. *Optics express*, 26(7):9039–9049, 2018.
7. Min Liu, Xu Yang, Ping Shum, and Hongtao Yuan. High-sensitivity birefringent and single-layer coating photonic crystal fiber biosensor based on surface plasmon resonance. *Applied optics*, 57(8):1883–1886.
8. Min Liu, Xu Yang, Bingyue Zhao, Jingyun Hou, and Ping Shum. Square array photonic crystal fiber-based surface plasmon resonance refractive index sensor. *Modern Physics Letters B*, 31(36):1750352, 2017.
9. AA Rifat, Ghafour Amouzad Mahdiraji, YM Sua, YG Shee, Rajib Ahmed, Desmond M Chow, and FR Maham Adikan. Surface plasmon resonance photonic crystal fiber biosensor: a practical sensing approach. *IEEE Photonics Technology Letters*, 27(15):1628–1631, 2015.
10. Ahmmed Rifat, GMahdiraji Chow, Yu Shee, Rajib Ahmed and Faisal Adikan. Photonic Crystal Fiber based surface plasmon resonance sensor with selective analyte channels and graphene silver deposited core. *Sensors*, 15(5):11499–11510, 2015.



P Vinod Kumar currently in final year pursuing Engineering in Electronics and Communication at SRM Institute of Science and Technology, Kattankulathur, Kancheepuram, Tamil Nadu.



S Nivash currently working as a Assistant Professor in School of ECE, SRM Institute of science and technology., Kattankulathur, Kancheepuram, Tamil Nadu.



Mohammed Fahimullah Acurrently in final year pursuing Engineering in Electronics and Communication at SRM Institute of Science and Technology, Kattankulathur, Kancheepuram, Tamil Nadu.



K Vinay Gokul currently in final year pursuing Engineering in Electronics and Communication at SRM Institute of Science and Technology, Kattankulathur, Kancheepuram, Tamil Nadu.